ISSN 1674-1056
http://cpb.iphy.ac.cn
http://iopscience.iop.org/cpb
中国物理 B
Chinese Physics
中国物理 Chinese Physics B

Importance of ligands on TiO_2 nanocrystals for perovskite solar cells

Yao Zhao(赵耀), Yi-Cheng Zhao(赵怡程), Wen-Ke Zhou(周文可), Rui Fu(伏睿), Qi Li(李琪), Da-Peng Yu(俞大鹏), Qing Zhao(赵清)
Citation: Chin. Phys. B . 2018, 27(1): 018401. **doi:** 10.1088/1674-1056/27/1/018401

Journal homepage: http://cpb.iphy.ac.cn; http://iopscience.iop.org/cpb

What follows is a list of articles you may be interested in

O_3 fast and simple treatment-enhanced p-doped in Spiro-MeOTAD for CH_3NH_3I vapor-assisted processed $CH_3NH_3PbI_3$ perovskite solar cells

En-Dong Jia(贾恩东), Xi Lou(娄茜), Chun-Lan Zhou(周春兰), Wei-Chang Hao(郝维昌), Wen-Jing Wang(王文静)
Chin. Phys. B . 2017, 26(6): 068803. **doi:** 10.1088/1674-1056/26/6/068803

Improving power conversion efficiency of perovskite solar cells by cooperative LSPR of gold-silver dual nanoparticles

Peng Liu(刘鹏), Bing-chu Yang(杨兵初), Gang Liu(刘钢), Run-sheng Wu(吴闰生), Chu-jun Zhang(张楚俊), Fang Wan(万方), Shui-gen Li(李水根), Jun-liang Yang(阳军亮), Yong-li Gao(高永立), Cong-hua Zhou(周聪华)
Chin. Phys. B . 2017, 26(5): 058401. **doi:** 10.1088/1674-1056/26/5/058401

Simulation design of P-I-N-type all-perovskite solar cells with high efficiency

Hui-Jing Du(杜会静), Wei-Chao Wang(王韦超), Yi-Fan Gu(顾一帆)
Chin. Phys. B . 2017, 26(2): 028803. **doi:** 10.1088/1674-1056/26/2/028803

Alleviating hysteresis and improving device stability of perovskite solar cells via alternate voltage sweeps

Chao Xia(夏超), Wei-Dong Song(宋伟东), Chong-Zhen Zhang(张崇臻), Song-Yang Yuan(袁松洋), Wen-Xiao Hu(胡文晓), Ping Qin(秦萍), Ru-Peng Wang(王汝鹏), Liang-Liang Zhao(赵亮亮), Xing-Fu Wang(王幸福), Miao He(何苗), Shu-Ti Li(李述体)
Chin. Phys. B . 2017, 26(1): 018401. **doi:** 10.1088/1674-1056/26/1/018401

Improving the performance of perovskite solar cells with glycerol-doped PEDOT:PSS buffer layer

Jian-Feng Li(李建丰), Chuang Zhao(赵创), Heng Zhang(张恒), Jun-Feng Tong(同军锋), Peng Zhang(张鹏), Chun-Yan Yang(杨春燕), Yang-Jun Xia(夏养君), Duo-Wang Fan(范多旺)
Chin. Phys. B . 2016, 25(2): 028402. **doi:** 10.1088/1674-1056/25/2/028402

SPECIAL TOPIC — New generation solar cells

Importance of ligands on TiO_2 nanocrystals for perovskite solar cells*

Yao Zhao(赵耀), Yi-Cheng Zhao(赵怡程), Wen-Ke Zhou(周文可), Rui Fu(伏睿), Qi Li(李琪), Da-Peng Yu(俞大鹏), and Qing Zhao(赵清)†

State Key Laboratory for Mesoscopic Physics and Electron Microscopy Laboratory, School of Physics, Peking University, Beijing 100871, *China*

(Received 27 September 2017; revised manuscript received 21 November 2017; published online 22 December 2017)

The fabrication of high-quality electron-selective layers at low temperature is a prerequisite to realizing efficient flexible and tandem perovskite solar cells (PSCs). A colloidal-quantum-dot ink that contains TiO_2 nanocrystals enables the deposition of a flat film with matched energy level for PSCs; however, the selection of ligands on the TiO_2 surface is still unexplored. Here, we systematically studied the effect of the titanium diisopropoxide bis(acetylacetonate) ($TiAc_2$) ligand on the performance of PSCs with a planar n–i–p architecture. We prepared TiO_2 nanocrystals from $TiCl_4$ and ethyl alcohol with Cl^- ligands attached on its surface and we found that a tiny amount of $TiAc_2$ treatment of as-prepared TiO_2 nanocrystals in a mixed solution of chloroform and methyl alcohol can enhance PSC power conversion efficiency (PCE) from 14.7% to 18.3%. To investigate the effect of $TiAc_2$ ligand on PSCs, TiO_2 samples with different $TiAc_2$ content were prepared by adding $TiAc_2$ into the as-obtained TiO_2 nanocrystal solution. We use x-ray photoelectron spectroscopy to identify the content of Cl so as to reveal that Cl ligands can be substituted by $TiAc_2$. We speculate that the improvement in PCE originates from amorphous TiO_2 formation on the TiO_2 nanocrystal surface, whereby a single-molecule layer of amorphous TiO_2 facilitates charge transfer between the perovskite film and the TiO_2 electronic transport layer, but excessive $TiAc_2$ lowers the PSC performance dramatically. We further prove our hypothesis by x-ray diffraction measurements. We believe the PCE of PSCs can be further improved by carefully choosing the type and changing the content of surface ligands on TiO_2 nanocrystal.

Keywords: $TiAc_2$, TiO_2 nanocrystal, surface ligand, perovskite solar cells

PACS: 84.60.Jt, 88.40.H–, 84.60.Bk **DOI:** 10.1088/1674-1056/27/1/018401

1. Introduction

The rapid progress of hybrid organic–inorganic metal halide perovskite solar cells PSCs represents a breakthrough for next-generation photovoltaic devices. Perovskite films possess many distinct properties such as tunable and suitable bandgap energy,[1–4] large dielectric constant,[5,6] long carrier diffusion lengths,[6–8] large absorption coefficient,[9–12] high carrier mobility,[12] and long carrier lifetime.[13] These special properties enable PSCs to be an ideal material as active layer of solar cells. Since Miyasaka *et al.*[14] reported PSCs for the first time, impressive progress has been made to promote their power conversion efficiency (PCE) from 3.8% to 22.1%.[15] To further optimize the PCE and stability of PSCs, many effective methods have been used such as changing electronic transport layer (ETL) materials, introducing additives, and using inverted device architecture.[16–27] Among all the ETLs in PSCs, TiO_2-based solar cells are always prone to achieving the highest PCE.[15] However, traditional perovskite TiO_2 ETL requires high-temperature (450 °C) processing, which is not only time-consuming and complex but also excludes the use of other substrates such as indium tin oxide (ITO) and flexible organic substrates.[28–30] Therefore, low-temperature TiO_2 nanocrystals are especially welcome, because they provide an opportunity to use flexible substrates to adopt roll-to-roll manufacturing of PSCs in the future.[31,32]

Yang *et al.* first invented low-temperature TiO_2 ETL by modifying TiO_2 nanocrystals dispersed in ethanol with YCl_3 and they reached then-record efficiency of 19.3%.[10] Tan *et al.* came up with a new strategy to modify TiO_2 nanocrystals with Cl^- ligand by dispersing nanocrystals into a mixed solution of chloroform and methyl alcohol (volume ratio 1:1). PSCs comprising Cl^- capped TiO_2 nanocrystal ETL reach efficiency greater than 20% and retain 90% of their initial performance after 500 h of continuous room-temperature operation at their maximum power point under one-sun illumination.[33] Kim *et al.* reported that an amorphous TiO_2 compact layer with a well-crystallized surface PSCs reached 9.97% efficiency, whereas pure amorphous TiO_2 ETL PSCs only have 1.73% PCE.[34] This discovery reminds us that it is the ETL surface rather than the bulk material that really affects the electron extraction. Dong *et al.* modified TiO_2 with WO_3 and they found that the photocurrent density increased dramatically.[35]

$TiAc_2$ is conventionally used as a dispersing agent to disperse TiO_2 nanocrystals in alcohol, but we think it is also a functional ligand that can enhance the electron extraction efficiency and thus lead to a great improvement in PSC performance. We systematically study the effect of $TiAc_2$ content on PSCs for the first time and reveal the mechanism behind

*Project supported by the National Natural Science Foundation of China (Grant Nos. 51622201, 61571015, and 91433102).

†Corresponding author. E-mail: zhaoqing@pku.edu.cn

© 2018 Chinese Physical Society and IOP Publishing Ltd

the change in PSC performance.

2. Experiment details

2.1. Materials

Methylammonium iodide, methylammonium bromine, and formamidine iodide were purchased from Dyesol. Lead iodide, lead bromide, N,N-dimethylformamide, hydrochloric acid, chlorobenzene, bis(trifluoromethane)sulfonamide lithium, 4-tert-butylpyridine, titanium tetraisopropoxide, and cesium iodide were purchased from Sigma-Aldrich. Spiro-OMeTAD was purchased from Lumtec. ITO was purchased from Thin Film Device Inc. All solid chemicals used in this experiment were 99.999% pure.

2.2. Synthesis of TiO_2 nanocrystals

The following experiments were all carried out in ambient environment. First, 2 mL $TiCl_4$ (99% Alfa-Aesar) was injected very slowly into 8 mL ethanol alcohol with 3000 rpm stirring speed to avoid local overheating of ethanol. The reaction vial was placed into an ice–water mixture. After 30 min, 40 mL of anhydrous benzyl alcohol was added to the previous solution and stirred for 10 min. The resulting solution was sealed in a vial and heated in an 80 °C water bath for approximately 10 h. The as-prepared TiO_2 nanocrystals were then precipitated from the as-obtained solution by the addition of 200 ml diethyl ether and isolated by centrifugation at 5000 rpm for 2 min. The solid was subsequently washed by adding anhydrous ethanol and diethyl ether (volume ratio 1:5), followed by an identical centrifugation process. This washing procedure was repeated twice. To obtain the Cl-ligand-capped TiO_2 colloidal solution, the washed TiO_2 nanocrystals were dispersed into anhydrous chloroform and anhydrous methanol (1:1 volume ratio). Finally, 5 μL/mL, 10 μL/mL, 50 μL/mL, 100 μL/mL, and 500 μL/mL $TiAc_2$ were separately added into 6 mg/ml TiO_2 nanocrystal solution.

2.3. Device fabrication

ITO substrates were cleaned with acetone and isopropanol in an ultrasonic bath, sequentially. These substrates were then spin-coated with as-obtained TiO_2 nanocrystals in solution at 3000 rpm for 30 s and annealed at 150 °C for 30 min on a hotplate. For the perovskite layer, a $Cs_{0.05}FA_{0.81}MA_{0.14}PbI_{2.55}Br_{0.45}$ precursor solution (1.4 M) was prepared with the molar ratios of $PbI_2/PbBr_2$ and FAI/MABr both fixed at 0.85:0.15, molar ratio of CsI/(FAI+MABr) = 0.05:0.95, and molar ratio of (FAI+MABr+CsI)/(PbI_2+$PbBr_2$) fixed at 1:1. The perovskite films were deposited onto the TiO_2 substrates with a two-step spin-coating procedure, i.e., 2000 rpm for 10 s with an acceleration of 200 rpm/s, followed by 5000 rpm for 40 s with a ramp-up of 1000 rpm/s. Chlorobenzene (100 μL) was dropped on the spinning substrate during the second spin-coating step, 10 s before the end of the procedure. To form a thick but still smooth perovskite film, chlorobenzene was slowly dropped on the precursor film within 3 s to allow sufficient extraction of extra DMSO through the entire precursor film. The substrate was then immediately transferred to a hotplate and held at 100 °C for 10 min. After cooling down to room temperature, the hole transport layer (HTL) was then coated on the sample. The precursor of the HTL was prepared by using 1 mL spiro-OMeTAD/chlorobenzene (90 mg/mL) solution with the addition of 15 mL Li-TFSI/acetonitrile (210 mg/mL), and 40 mL TBP. Finally, 100 nm gold was deposited as a bottom electrode by thermal evaporation under a pressure of 8×10^{-6} Pa.

2.4. Photovoltaic characterization

The current density–voltage (J–V) curves were measured using an Agilent B2912 source–measure unit under AM1.5G illumination at 100 mW/cm^2 provided by a Zolix simulator in an ambient environment. The active area was 0.049 cm^2.

3. Results and discussion

Figures 1(a)–1(d) show top-view scanning electron microscopy (SEM) images of the TiO_2 nanocrystals ETL with different $TiAc_2$ ligand content. We spin-coated TiO_2 nanocrystal ink three times to ensure good coverage. All the TiO_2 ETL samples cover the ITO perfectly, suggesting ligand content would not have identifiable effect on the coverage of the TiO_2 layer, and excluding the possibility that PCE variation stems from ETL coverage. It is found that the granular sensation of TiO_2 nanocrystals decays with the increase in $TiAc_2$ ligand content. We speculate that some amorphous TiO_2 is formed because the low annealing temperature (150 °C) is unable to transform $TiAc_2$ into TiO_2 crystal. The morphologies of the perovskite films are the same on different TiO_2 ETLs (Fig. 1(f)).

As shown in Fig. 2(a), the cross-sectional SEM image indicates the presence of the TiO_2 ELT (50 nm), perovskite active layer (600 nm), spiro-OMeTAD HTL (120 nm), and Au electrode. Figures 2(a) and 1(f) suggest that a dense-grained uniform morphology with grain sizes around 500 nm was formed in all samples. It can be seen that the photovoltaic performance was dramatically enhanced for the solar cells with 10 μL/mL $TiAc_2$ addition (Fig. 2(b)). When 5 μL/mL $TiAc_2$ is added, the device short-circuit current density (J_{sc}) increases from 21.43 mA/cm^2 to 22.45 mA/cm^2; the device PCE increases from 14.52% to 17.74%; then, when the $TiAc_2$ additive increases to 10 μL/mL, J_{sc} increases to 22.6 mA/cm^2, the open-circuit voltage (V_{oc}) increases markedly from 0.972 V to 1.08 V, the fill factor (FF) increases to 75.22%, and PCE increases to 18.36%. The device PCE as a function of $TiAc_2$ content is shown in Fig. 2(c), and the detailed photovoltaic performance parameters are summarized in Table 1. A detailed discussion of these parameters will be presented later. Excessive $TiAc_2$ addition results in significant drops in FF and J_{sc}, indicating there is a problem at the perovskite/TiO_2 ETL interface.

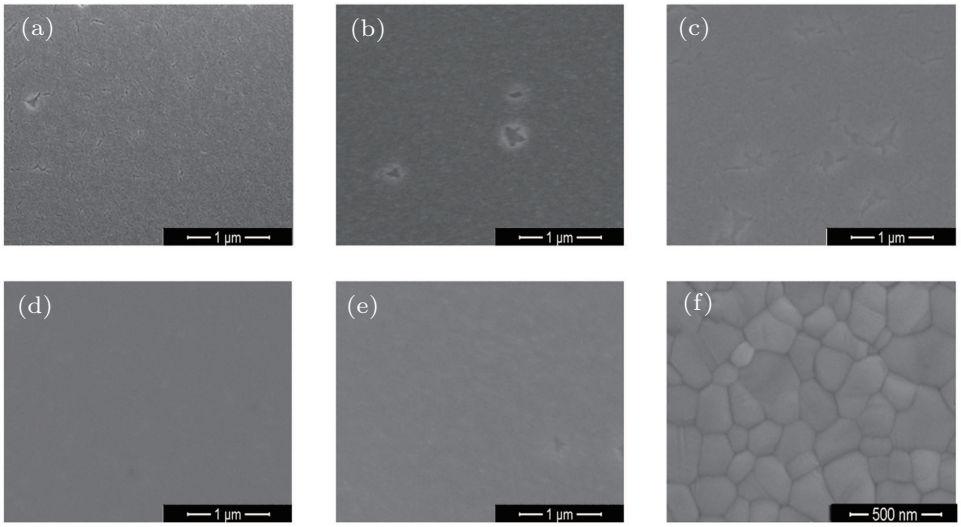


Fig. 1. Top-view SEM images of TiO_2 ETL with different $TiAc_2$ addition (a) 5 μL/mL, (b) 10 μL/mL, (c) 50 μL/mL, (d) 100 μL/mL, (e) 500 μL/mL, and (f) perovskite film.

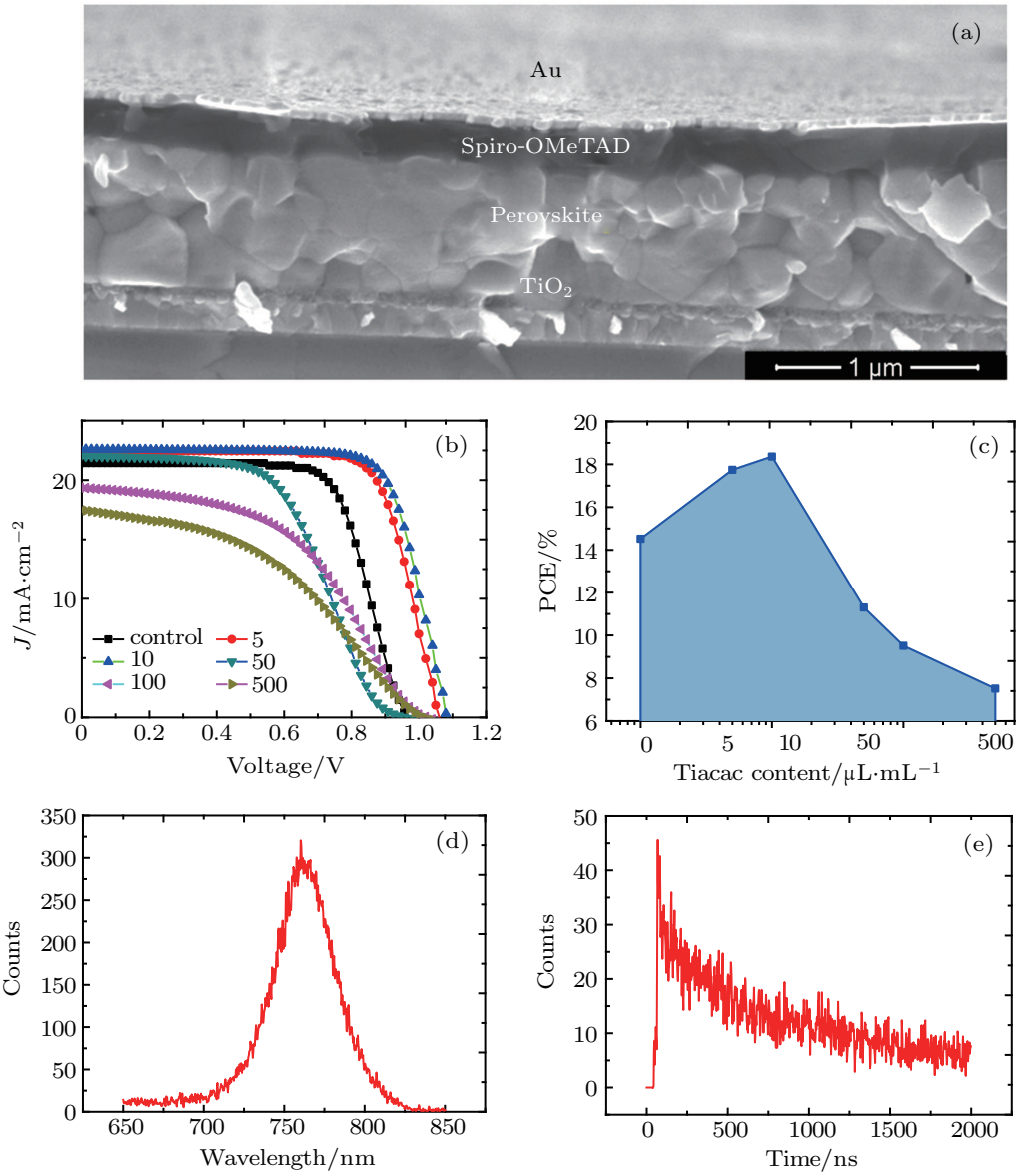


Fig. 2. (color online) (a) Cross-section SEM image of perovskite solar cells. (b) *I–V* curves of perovskite solar cells with different $TiAc_2$ content. (c) PCE changes with $TiAc_2$ addition variation. (d) Steady-state PL spectra of perovskite film on glass substrate. (e) Time-resolved PL decay spectra.

Table 1. PSCs performance parameters with different $TiAc_2$ addition.

$TiAc_2$ addition/μL·mL^{-1}	PCE/%	J_{sc}/mA·cm^{-2}	V_{oc}/V	FF/%
0	14.52	21.43	0.972	67.71
5	17.74	22.45	1.07	73.87
10	18.36	22.60	1.08	75.22
50	11.30	22.04	0.956	53.65
100	9.51	19.37	1.02	48.16
500	7.52	17.50	1.02	42.10

Steady-state photoluminescence (PL) spectra (Fig. 2(d)) indicate that the central wavelength is 780 nm, corresponding to a bandgap of 1.59 eV, which proves the perovskite active layer composition is $FA_{0.85}MA_{0.15}PbI_{2.55}Br_{0.45}$. We use time-resolved PL decay to further identify the film quality on glass substrate (Fig. 2(e)). The lifetime of the as-prepared perovskite film is approximately 1 μs, suggesting its high quality.

X-ray photoelectron spectroscopy (XPS) measurements reveal the composition of the films prepared by TiO_2 nanocrystals (Fig. 3(a)). Figure 3(d) indicates that the C 1s binding energy is centered at 285.3 eV, which deviates from the standard 284.6 eV, originated from electrons accumulated on the TiO_2 surface, resulting in a general shift in the XPS spectra. Taking this shift into account, we obtain the Ti $2p^{1/2}$ central at 458.8 eV and Ti $2p^{3/2}$ at 464.5 eV, respectively, which confirms the existence of TiO_2 (Fig. 3(c)). Now, we turn to Cl^- and obtain the XPS spectra for different $TiAc_2$ addition samples. The XPS results presented in Fig. 3(b) were normalized to the Ti counts in order to exclude the effect of different samples with different Ti signals. It was found that the control sample without $TiAc_2$ addition shows a strong signal of Cl $2p^{1/2}$ at 198.7 eV and $2p^{3/2}$ 198.9 eV after correction for the general shift. However, after adding 5 μL/mL $TiAc_2$ into TiO_2 chloroform and methyl alcohol mixed solution (6 mg/mL), the Cl signal suddenly disappears, to say nothing of the 10 μL/mL, 50 μL/mL, 100 μL/mL, and 500 μL/mL $TiAc_2$ additions. The interaction between $TiAc_2$ and TiO_2 nanocrystals is so strong that almost all the Cl^- ligands desorbed from the $TiAc_2$ surface after addition.

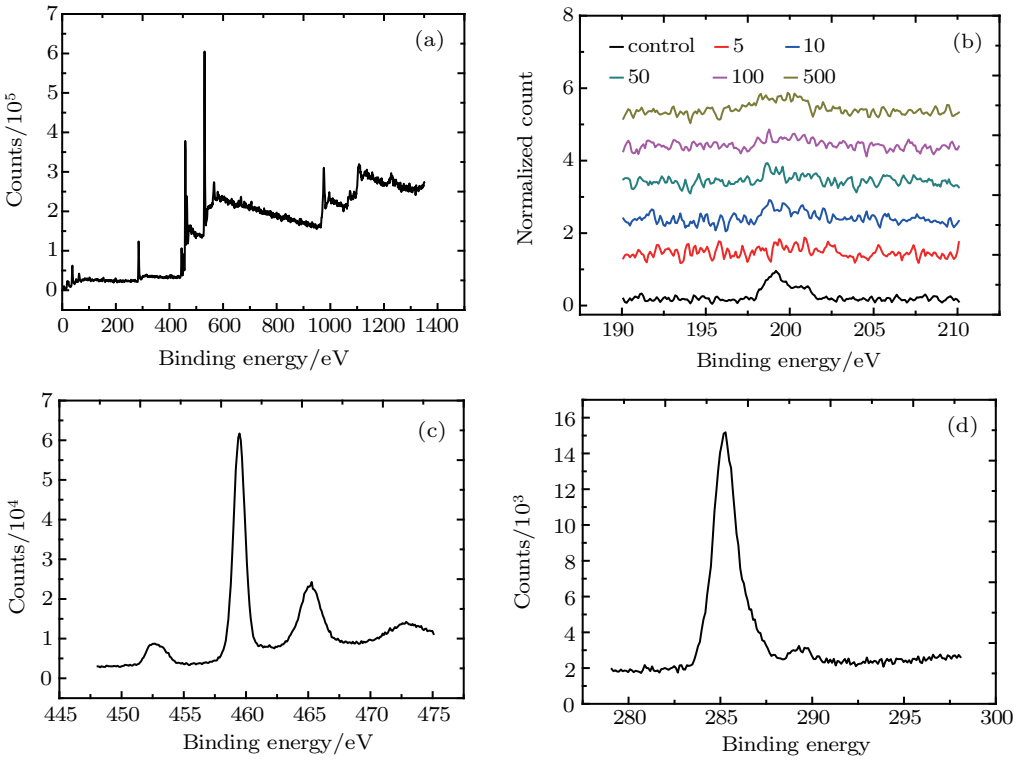


Fig. 3. (color online) (a) General XPS spectra of TiO_2 nanocrystals. (b) Cl 2p XPS spectra of TiO_2 nanocrystals with different $TiAc_2$ content (μL/mL). (c) Ti 2p XPS spectra. (d) C1s XPS spectra.

We surmise that the annealing temperature of 150 °C is insufficient to transfer $TiAc_2$ into TiO_2 crystals, because $TiAc_2$ is the raw material for high-temperature pyrolysis of TiO_2 at 450 °C. It is probable that under 150 °C, $TiAc_2$ transforms into amorphous TiO_2 with a bandgap between TiO_2 nanocrystals and perovskite film. TiO_2 nanocrystals are approximately 5 nm in diameter, and TiO_2 lattice length is 0.2 nm. Assuming a cubic shape of TiO_2 nanocrystals, we calculate that each nanocrystal contains 15625 TiO_2 lattice points and 3125 lattice surfaces. Then, we can roughly estimate the coverage of 10 μL/mL $TiAc_2$. The $TiAc_2$ molecular density is approximately 1.6×10^{19} mL^{-1}; 1 mL spin-coated TiO_2 solution has 1.125×10^{19} lattice surface; considering the strong interaction between TiO_2 and $TiAc_2$, the TiO_2 nanocrystal will be covered by a single-molecule layer of $TiAc_2$. Once these modified TiO_2 nanocrystals experience 150 °C annealing, amorphous TiO_2 forms on the surface. The single-molecule layer of amorphous TiO_2 with a bandgap between perovskite and

TiO_2 ETL facilitates electron transfer by lowering the barrier between the perovskite film and ETL, which explains why the PCE and FF increase when adding $TiAc_2$ into TiO_2 solution. V_{oc} will increase as well owing to better carrier transportation and reduced carrier recombination. We performed an ultraviolet photoelectron spectroscopy (UPS) measurement to prove our hypothesis. As shown in Fig. 4, the work function of TiO_2 increases from 5.65 eV to 5.86 eV after $TiAc_2$ addition, indicating that the conduction band of $TiAc_2$-modified TiO_2 nanocrystals becomes 0.21 eV lower than the pristine TiO_2 nanocrystals, and thus lowers the barrier between the perovskite and ETL. However, the newly formed TiO_2 is essentially amorphous with relatively high series resistance and defect density; excessive amorphous TiO_2 will inevitably impact the PSC performance.

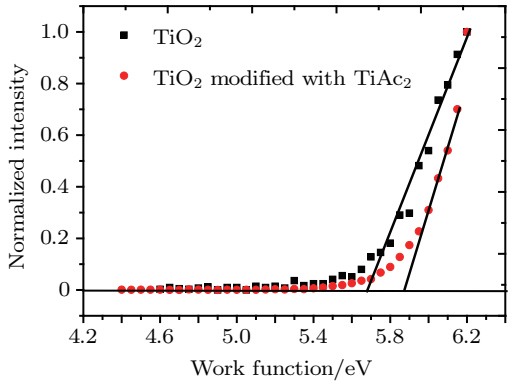


Fig. 4. (color online) UPS measurement of TiO_2 and $TiAc_2$-modified TiO_2 film.

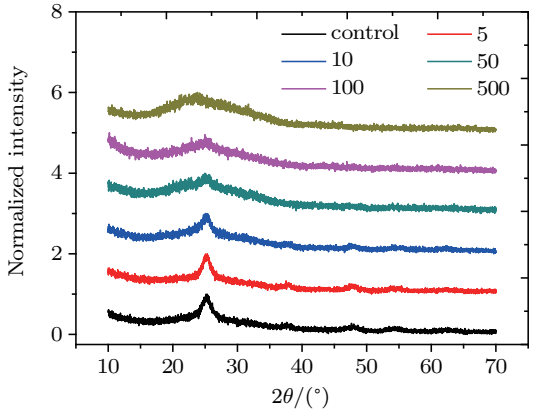


Fig. 5. (color online) XRD pattern of TiO_2 with different $TiAc_2$ addition (unit: μL/mL).

We use x-ray diffraction (XRD) measurements to prove our scenario; $2\theta = 25.325°$ is ascribed to the anatase phase of TiO_2 (Fig. 5). The intensity of the XRD signal decays with $TiAc_2$ addition; when the $TiAc_2$ addition reached 500 μL/mL, the signal of anatase TiO_2 disappeared. This strongly suggests that amorphous TiO_2 formed during the 150 °C annealing process. The XRD intensity of TiO_2 film is still obvious with 10 μL/mL $TiAc_2$ addition, because the single-molecule layer amorphous TiO_2 is insufficient to screen the signal of the well crystalized TiO_2. However, when excessive $TiAc_2$ is added, the XRD signal intensity decays precipitously.

4. Conclusion and perspectives

In summary, we confirm that 10 μL/mL $TiAc_2$ as an additive to TiO_2 nanocrystals in a mixed solution of chloroform and methyl alcohol (6 mg/mL) enhances the PCE of PSCs from 14.52% to 18.36%. We propose a mechanism behind the enhanced PSC performance: when adding 10 μL/mL $TiAc_2$ into as-prepared TiO_2 solution, Cl^- will be replaced by $TiAc_2$ and the attached $TiAc_2$ will transform to a single-molecule layer of amorphous TiO_2, the bandgap of which is between perovskite and TiO_2 nanocrystals. This lowers the barrier between the perovskite and ETL, and facilitates electron transport. However, when excessive (> 50 μL/mL) $TiAc_2$ is added, the FF and J_{sc} drop dramatically because the thickness and defect density of the newly formed amorphous TiO_2 are so high that the electron transport between the perovskite and ETL is blocked. These results indicate that the PSC performance can be further optimized by carefully choosing other ligands and controlling their content.

References

[1] Papavassiliou G C 1996 *Molecular Crystals and Liquid Crystals Science and Technology. Section A. Molecular Crystals and Liquid Crystals* **286** 231
[2] Mei A, Li X, Liu L, Ku Z, Liu T, Rong Y, Xu M, Hu M, Chen J, Yang Y, Grätzel M and Han H 2014 *Science* **345** 295
[3] Zhang W, Anaya M, Lozano G, Calvo M E, Johnston M B, Míguez H and Snaith H J 2015 *Nano Lett.* **15** 1698
[4] Hao F, Stoumpos C C, Cao D H, Chang R P H and Kanatzidis M G 2014 *Nat. Photon.* **8** 489
[5] Stranks S D, Eperon G E, Grancini G, Menelaou C, Alcocer M J P, Leijtens T, Herz L M, Petrozza A and Snaith H J 2013 *Science* **342** 341
[6] Snaith H J 2013 *J. Phys. Chem. Lett.* **4** 3623
[7] Heo J H, Im S H, Noh J H, Mandal T N, Lim C-S, Chang J A, Lee Y H, Kim H J, Sarkar A, NazeeruddinMd K, Gratzel M and Seok S I 2013 *Nat. Photon.* **7** 486
[8] Chen W, Wu Y, Yue Y, Liu J, Zhang W, Yang X, Chen H, Bi E, Ashraful I, Gratzel M and Han L 2015 *Science* **350** 944
[9] Yang W S, Noh J H, Jeon N J, Kim Y C, Ryu S, Seo J and Seok S I 2015 *Science* **348** 1234
[10] Zhou H, Chen Q, Li G, Luo S, Song T B, Duan H S, Hong Z, You J, Liu Y and Yang Y 2014 *Science* **345** 542
[11] Li Y, Cooper J K, Liu W, Sutter-Fella C M, Amani M, Beeman J W, Javey A, Ager J W, Liu Y, Toma F M and Sharp I D 2016 *Nat. Commun.* **7** 12446
[12] Shi D, Adinolfi V, Comin R, Yuan M, Alarousu E, Buin A, Chen Y, Hoogland S, Rothenberger A, Katsiev K, Losovyj Y, Zhang X, Dowben P A, Mohammed O F, Sargent E H and Bakr O M 2015 *Science* **347** 519
[13] Kim H S, Lee C R, Im J H, Lee K B, Moehl T, Marchioro A, Moon S J, Humphry-Baker R, Yum J H, Moser J E, Grätzel M and Park N G 2012 *Sci. Rep.* **2** 591
[14] Kojima A, Teshima K, Shirai Y and Miyasaka T 2009 *J. Am. Chem. Soc.* **131** 6050
[15] Yang W S, Park B W, Jung E H, Jeon N J, Kim Y C, Lee D U, Shin S S, Seo J, Kim E K, Noh J H and Seok S I 2017 *Science* **356** 1376
[16] Cao J, Yin J, Yuan S, Zhao Y, Li J and Zheng N 2015 *Nanoscale* **7** 9443
[17] Lee J W, Kim H S and Park N G 2016 *Acc. Chem. Res.* **49** 311

[18] Wang Z, Xia Y, Chen Y and Huang W 2017 *J. Mater. Chem. A* **5** 12602
[19] Li X, Dar M I, Yi C, Luo J, Tschumi M, Zakeeruddin S M, Nazeeruddin M K, Han H and Gratzel M 2015 *Nat. Chem.* **7** 703
[20] Qin C, Matsushima T, Fujihara T and Adachi C 2017 *Adv. Mater.* **29** 1603808
[21] Quan L N, Yuan M, Comin R, Voznyy O, Beauregard E M, Hoogland S, Buin A, Kirmani A R, Zhao K, Amassian A, Kim D H and Sargent E H 2016 *J. Am. Chem. Soc.* **138** 2649
[22] Rong Y, Hou X, Hu Y, Mei A, Liu L, Wang P and Han H 2017 *Nat. Commun.* **8** 14555
[23] Si H, Liao Q, Kang Z, Ou Y, Meng J, Liu Y, Zhang Z and Zhang Y 2017 *Adv. Function. Mater.* **27** 1701804
[24] Wu Y, Xie F, Chen H, Yang X, Su H, Cai M, Zhou Z, Noda T and Han L 2017 *Adv. Mater.* **29** 1701073
[25] Zhang J, Hu Z, Huang L, Yue G, Liu J, Lu X, Hu Z, Shang M, Han L and Zhu Y 2015 *Chem. Commun.* **51** 7047
[26] Zuo C and Ding L 2014 *Nanoscale* **6** 9935
[27] Xu L G, Qiu W, Chen R F, Zhang H M and Huang W 2018 *Acta Phys. Chim. Sin.* **34** 36
[28] You J, Hong Z, Yang Y, Chen Q, Cai M, Song T B, Chen C C, Lu S, Liu Y, Zhou H and Yang Y 2014 *ACS Nano* **8** 1674
[29] Shin S S, Yang W S, Noh J H, Suk J H, Jeon N J, Park J H, Kim J S, Seong W M and Seok S I 2015 *Nat. Commun.* **6** 7410
[30] Chhowalla M, Tretiak S, Alam M A, Wang H L and Mohite A D 2015 *Science* **347** 522
[31] Nie W, Tsai H, Asadpour R, Blancon J C, Neukirch A J, Gupta G and Crochet J J 2003 *J. Am. Chem. Soc.* **125** 14539
[32] Docampo P, Ball J M, Darwich M, Eperon G E and Snaith H J 2013 *Nat. Commun.* **4** 2761
[33] Tan H, Jain A, Voznyy O, Lan X, García de Arquer F P, Fan J Z, Quintero-Bermudez R, Yuan M, Zhang B, Zhao Y, Fan F, Li P, Quan L N, Zhao Y, Lu Z H, Yang Z, Hoogland S and Sargent E H 2017 *Science* **355** 722
[34] Kim I S, Haasch R T, Cao D H, Farha O K, Hupp J T, Kanatzidis M G and Martinson A B F 2016 *ACS Appl. Mater. Interf.* **8** 24310
[35] Wang W G, Zhu L, Weng Y Y and Dong W 2017 *Chin. Phys.* **34** 028201